



Expression dynamics and a loss-of-function of *Arabidopsis RabC1* GTPase unveil its role in plant growth and seed development

Uzma Khatoon^{1,2} · Vivek Prasad² · Samir V. Sawant¹

Received: 18 November 2022 / Accepted: 16 March 2023 / Published online: 29 March 2023
© The Author(s), under exclusive licence to Springer-Verlag GmbH Germany, part of Springer Nature 2023

Abstract

Main conclusion Transcript isoform dynamics, spatiotemporal expression, and mutational analysis uncover that *Arabidopsis RabC1* GTPase is required for root length, flowering time, seed size, and seed mucilage.

Abstract Rab GTPases are crucial regulators for moving different molecules to their specific compartments according to the needs of the cell. In this work, we illustrate the role of RabC1 GTPase in *Arabidopsis* growth and seed development. We identify and analyze the expression pattern of three transcript isoforms of *RabC1* in different development stages, along with their tissue-specific transcript abundance. The promoter activity of *RabC1* using promoter-GUS fusion shows that it is widely expressed during the growth of *Arabidopsis*, particularly in seed tissues such as chalazal seed coat and chalazal endosperm. Lack of RabC1 function led to shorter roots, lesser biomass, delayed flowering, and sluggish plant development. The mutants had smaller seeds than the wildtype, less seed mass, and lower seed coat permeability. Developing seeds also revealed a smaller endosperm cavity and shorter integument cells. Additionally, we found that the knock-out mutant had downregulated expression of genes implicated in the transit of sugars and amino acids from maternal tissue to developing seed. The seeds of the loss-of-function mutant had reduced seed mucilage. All the observed mutant phenotypes were restored in the complemented lines confirming the function of RabC1 in seed development and plant growth.

Keywords Chalazal endosperm · Chalazal seed coat · Seed mucilage · Seed size · Transcript isoforms

Abbreviations

DAG	Day after germination
DAP	Day after pollination
UMAMIT	Usually multiple acids move in an out transporter

Introduction

Membrane trafficking is essential for a number of cellular processes in plant growth and development, such as the manufacture of cell walls, uptake of nutrients, hormone signaling, and various other cell activities (Geldner et al. 2001; Takano et al. 2005; Harpaz-Saad et al. 2011). The communication between different cell compartments is mediated by membrane trafficking, a crucial process for transporting molecules. Membrane trafficking functions through various steps comprising budding, transport, targeting, tethering, and vesicle fusion via effector proteins to the target organelles (Zerial and McBride 2001). Spatiotemporal regulation and specificity of membrane trafficking during development and various cellular activities are mainly mediated by Rab GTPases, belonging to the family of small GTPases (Stenmark 2009; Ebine 2015; Gu et al. 2020).

Rab GTPases represent a molecular switch, and their regulatory module relies on the GTP-binding and hydrolysis process. Rab GTPases are operative when associated with GTP, and upon hydrolysis, they become inactive (Stenmark

Communicated by Dorothea Bartels.

✉ Samir V. Sawant
samirsawant@nbri.res.in

¹ Plant Molecular Biology and Biotechnology Division, CSIR-National Botanical Research Institute, Rana Pratap Marg, Lucknow 226001, India

² Department of Botany, University of Lucknow, Lucknow 226007, India

et al. 1994; Markgraf et al. 2007). The activation, as well as inactivation of Rab GTPases, depends on the particular guanine nucleotide exchange factors (GEFs) and GTPase-activating proteins (GAPs) (Olkonen and Stenmark 1997; Pereira-Leal and Seabra 2001; Vernoud et al. 2003; Woollard and Moore 2008). In Arabidopsis, 57 Rab GTPases are reported that are divided into eight clades, namely, RabA/Rab11, RabB/Rab2, RabC/Rab18, RabD/Rab1, RabE/Rab8, RabF/Rab5, RabG/Rab7, and RabH/Rab6 based on their similarity with the yeast and the animal GTPases (Pereira-Leal and Seabra 2001; Rutherford and Moore 2002; Nielsen 2020). Numerous plant Rab GTPases of the different groups are predicted to be localized to a distinct compartment in various stages of membrane trafficking. Proteins belonging to RabB and RabD have been involved in the initial phases of trafficking to Golgi-associated structures, whereas members of RabF (RabF1 and RabF2) and RabG3 subclass have been associated with transport to the vacuole (Batoko et al. 2000; Rojo et al. 2001; Cheung et al. 2002; Vernoud et al. 2003; Woollard and Moore 2008; Nielsen 2020). Several pieces of research have revealed the role of Rab GTPases, mainly belonging to RabA, RabE, and RabF clades, in post-Golgi secretory and endocytic processes (Zheng et al. 2005; Foucart et al. 2008; Huang et al. 2021). Members of the RabH clade, such as RabH1b and RabH1c, have been implicated in the trafficking between Golgi and plasma membrane (He et al. 2018; Jia et al. 2018). The RabC family in plants is closest to the Rab18 GTPase-like family of animals, and RabC2a of this family seems to recruit myosin motors to peroxisomes (Hashimoto et al. 2008).

Since the discovery, numerous Rab GTPases have been known to play a crucial role in plant growth, plant–microbe interaction, biotic stress, drought stress, and adaptation processes (Kotzer et al. 2004; Szumlanski and Nielsen 2009; Ambastha et al. 2021; Huang et al. 2021). In Arabidopsis, RabH1b appears to be involved in cellulose biosynthesis during hypocotyls growth by engaging in the trafficking of CELLULOSE SYNTHASE 6 (CESA6) across intracellular compartments to the plasma membrane (He et al. 2018). Further, a mutation in *RabA5c* disturbs cell geometry during lateral organ development suggesting its role in wall stiffening and cell shape (Kirchhelle et al. 2016). RabE1 seems to be implicated in exocytosis and PIN2-GFP endocytosis by interacting with SCD1(STOMATAL CYTOKINESIS DEFECTIVE 1 and SCD2 (Mayers et al. 2017). Rab GTPases also play a critical role in pollen development and the polarized growth of pollen tubes (Cheung et al. 2002). Specifically, RabD along with RabA appears to be involved in these processes (De Graaf et al. 2005; Peng et al. 2011). A lack of RabA4d activity leads to abnormalities in pollen tube growth polarization due to impairment in delivering the components essential for pollen tube growth. Also, it shows decreased pollen tube guidance towards micropyle

(Szumlanski and Nielsen 2009). *RabA4b* is expressed explicitly at the apex of developing root hair cells during cell expansion and is implicated in releasing cell wall elements required to expand the tip (Preuss et al. 2004). A double mutant of *AtRabD2b* and *AtRabD2c* genes has deformed pollen, furcate and swollen pollen tube ends and produces smaller siliques than the wildtype (Peng et al. 2011). We asked which RabGTPases are explicitly expressed in the seed and its function during seed development.

Seed development commences with double fertilization, producing a diploid embryo and triploid endosperm. The embryo is formed after several cell divisions, elongation, and differentiation, while the endosperm developmental progression involves the coenocyte phase, cellularization, and differentiation of cells (Wang et al. 2021). In Arabidopsis, expansion and growth of the embryo rely on endosperm breakdown, which is regulated by the endosperm-specific gene, *ZHOUPI* (Denay et al. 2014). Embryo and endosperm development coupled with the development of integument that later turns to mature seed coat after differentiation, pigments accumulation, and cell death. For a proper seed formation, these three structures must coordinate through cell–cell communications that require the secretion of signaling molecules (Wang et al. 2021).

This study focused on a Rab GTPase, which is involved in plant growth and seed development. Based on its high seed-preferential expression, we selected the RabC1 GTPase. Isoform identification, transcript abundance analysis, tissue-specific localization via GUS transcriptional fusion, and mutants' analysis implicate its contribution to cellular functions required for plant growth and seed formation.

Materials and methods

Plant materials, growth condition and transformation

Arabidopsis thaliana Col-0 plants were grown on autoclaved soilrite under long-day conditions (22 °C, 16 h light, 8 h dark) after three days of stratification of seeds at 4°C. For the seedling experiment, sterilized seeds, after three days of stratifications at 4°C, were germinated on a 0.7% agar medium comprising 0.5 × Murashige and Skoog salts (Sigma, St. Louis, MO, USA) at pH 5.75 for 5–6 days; after that five seedlings of each genotype in six replicates were transferred on square plates containing 0.8% agar medium, transferred to growth chamber and placed vertically. For the *RabC1_{prom}*:*GUS* reporter line, the construct was transformed in the *Agrobacterium* GV3101 strain, and plant transformation was done on the Col-0 background using the floral dipping method (Clough and Bent 1999). Seeds were grown on selection media containing 50 µg/ml of kanamycin.

RNA extraction, cDNA synthesis, and expression analysis

Total RNA was extracted from the different plant stages: mature leaf, rosette 30-day-old, stem, flower, bud, and root, and various stages of developing seeds, 3 days after pollination (DAP), 4DAP, 5DAP, 6DAP, 8DAP, 10DAP, and 16DAP siliques. According to the manufacturer's instructions, RNA was extracted utilizing Sigma spectrum™ total RNA kit and then subjected to DNase treatment (TURBO™ DNase kit; Ambion, Austin, TX, USA). Using Superscript III (Invitrogen, Waltham, MA, USA), first-strand complementary DNA (cDNA) was created from 2 µg of total RNA subjected to DNase treatment. The PCR was carried out using a Fast SYBR™ Green Master Mix (Applied Biosystems, Waltham, MA, USA) on an ABI 7500 Fast Real-Time PCR Machine (Applied Biosystems). The experiment used at least two distinct biological and 2–3 technical replicates. Relative expression was determined using the $2^{-\Delta\Delta Ct}$ method (Livak and Schmittgen 2001). Ubiquitin 10 was taken as an endogenous reference gene.

For the determination of the expression level of genes involved in seed size and seed filling for the validation of seed phenotypes (*UMAMIT25*, *UMAMIT24*, *CYP714A*, *CYCB1-4*, *SWEET11*, and *SWEET15*) in Col-0 and *rabc1-2*, RNA was extracted from the seeds dissected from 25 to 30 5DAP siliques of each genotype in two biological replicates. In addition, ubiquitin 10 and actin were taken as reference genes. The primer sequences are listed in Supplementary Table S1.

Plasmid construction and *in-silico* promoter analysis

To generate the *RabC1_{prom}::GUS* reporter line, 1202 bp promoter sequence from the upstream region of ATG was amplified and cloned into the pBluescript SK(+). From the sequenced clone, the HindIII and BamHI digested promoter region was ligated into the pBI121 binary vector (Chen et al. 2003) in front of the *GUS* gene. Primer sequences for cloning were given in Supplementary Table S1. *Agrobacterium*-mediated transformation in *Arabidopsis* Col-0 was performed as mentioned above. A minimum of seven lines were analyzed, and all showed consistent results. Two lines with single T-DNA insertion showing a 1:3 Mendelian segregation pattern were taken for the experiment.

For the analysis of the cis-regulatory motif in the promoter of *RabC1*, sequences were scanned in PlantCARE and PLACE (Higo et al. 1999; Lescot et al. 2002). In addition, the promoter's diagrammatic representation of selected cis-regulatory motifs was done using TB tools (Chen et al. 2020).

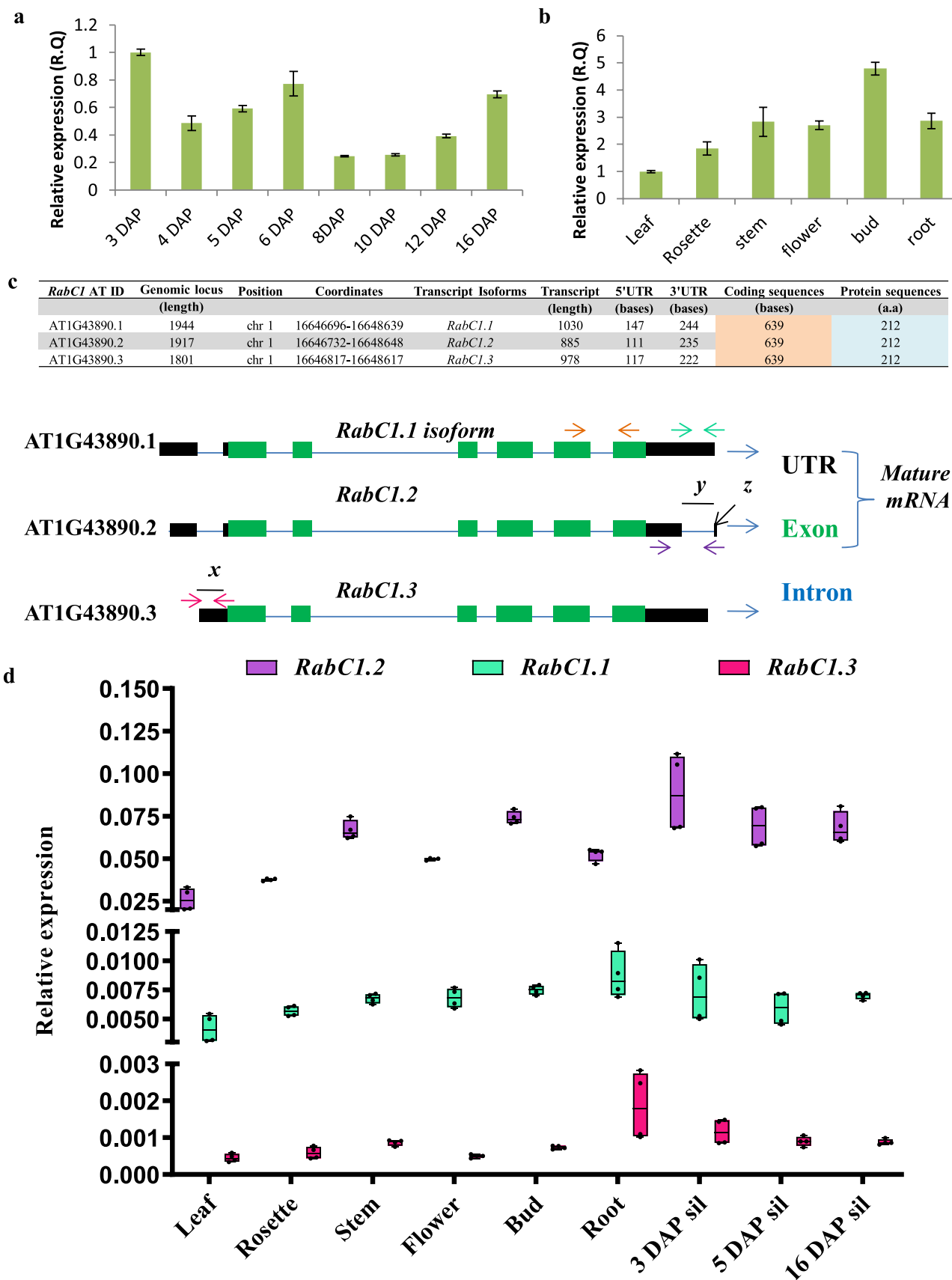
Histochemical GUS staining and quantitative fluorimetry assay

The spatiotemporal expression of *AtRabC1* in the *RabC1_{prom}::GUS* lines was analyzed by GUS staining (Jefferson et al. 1987), with a few alterations by adding 2 mM each of potassium ferrocyanide and potassium ferricyanide. Samples were incubated at 37 °C for 12–16 h and then cleared in a series of ethanol. Images were captured under a stereomicroscope (Leica microsystem). To detect the staining in the seed, freshly harvested siliques of a particular stage were slit longitudinally. Dissected seeds were incubated overnight in a GUS staining solution at 37 °C. After incubation and clearing in 1:2 acetic acid: ethanol and chloral hydrate solution, images were visualized under the light microscope (Leica microsystem).

GUS activity was quantified in plant extracts (Jefferson et al. 1987). In brief, 15-day-old seedlings (12–15 mg) (with and without induction of GA3 and salicylic acid, SA) in 3–8 replicates were crushed in 0.2 ml of GUS extraction buffer (50 mM Na₂HPO₄ pH-7.0, 10 mM DTT, 1 mM EDTA, 0.1% SLS, 0.1% Triton X-100) with micropestle in 1.5 ml Eppendorf tubes at 4°C. Tissue extracts were centrifuged at 16,200 g for 20 min at 4 °C. The supernatant was collected into fresh tubes. Then, 90 µl of the extract was mixed with 10 µl of 10X GUS assay buffer [4-methylumbelliferyl-β-D-glucuronide (MUG) suspended in GUS extraction buffer] and incubated at 37 °C for 2 h. After that, the reaction was terminated by adding 900 µl of 0.2 M sodium carbonate solution and was mixed adequately by vortexing. The reaction mixture was 2 times diluted. Fluorescence was measured using a Tecan spectrofluorometer with an excitation of 365 nm and emission at 455 nm. The specific GUS activity was calculated as nM 4-methylumbelliferone (MU) min⁻¹ mg protein⁻¹. Total protein was estimated using Bio-Rad dye.

Mutant characterization and genotyping

We obtained two T-DNA insertion lines, SALK_114305C (*rabc1-1*) and SALK_012129 (*rabc1-2*), from ABRC. The T-DNA in *rabc1-1* was positioned in the promoter, 335 nucleotides upstream of the translational start site. The T-DNA in *rabc1-2* was inserted in the intron, as mentioned in the figure (cf. Supplementary Fig. S7b). In both mutants, the left border was situated towards the 5' end of the gene. The T-DNA insertions and homozygosity were confirmed using a combination of primers (cf. Supplementary Fig. S7b, c, and d).



◀Fig. 1 Expression profile of *RabC1*. **a** qRT-PCR validation of *RabC1* transcript in different seed developing stages: 3 DAP, 4 DAP, 5 DAP, 6 DAP, 8 DAP, 10 DAP, 12 DAP, and 16 DAP siliques (primers designed from the exonic region, indicated by orange color arrows). A total of six replicates were taken (two biological and three technical replicates). Error bars denote the standard error (SE). **b** Relative expression of *RabC1* in different tissues: leaf, rosette, stem, flower, bud, and root. Error bars denote SE. Four replicates were taken (two biological and two technical replicates). **c** Gene structure and diagrammatic representation of transcript isoforms of *RabC1*. The black, blue, and green boxes represent the UTRs, introns, and exons (different color arrows represent the primers for different isoforms; common primers which recognize all three variants are indicated by orange arrows). The x indicates the portion of intron retained in the *RabC1.3* isoform, y represents the region of intron spliced out in the *RabC1.2* transcript, and z is denoted by the six extra adenine in the *RabC1.2* transcript isoform. **d** Relative expression for three transcript isoforms of *RabC1* in different vegetative and reproductive tissues: leaf, rosette, stem, flower, bud, root, 3 DAP siliques, 5 DAP siliques, and 16 DAP siliques. A total of four replicates were taken (two biological and two technical replicates)

Root length, seed mass, and seed size measurement

For comparative quantitative analysis of root length, plates were photographed, and root length was measured using ImageJ software. Boxplots were generated using Graph Pad Prism 8.4.2.

Mature, dry seeds were collected from the homozygous plants, and the weight of 250 seeds per aliquot of five different replicates was measured in each genotype. To determine seed size variables, seeds of multiple genotypes were photographed under a stereomicroscope at identical magnification. ImageJ software measured the area, perimeter, length, width, and length/width ratio of seeds. Boxplots were plotted in GraphPad Prism 8.4.2 software. Two-tailed Student's *t*-test and one-way ANOVA were carried out in excel and GraphPad Prism.

Differential interference contrast microscopy of developing seeds

The differences in the internal structure of seeds at different developing stages were analyzed, individual open flowers (marked as zero DAP) were tagged, and self-fertilized siliques of desired stages were collected, cut on both ends, slit longitudinally, and opened to dissect the seeds. Seeds were fixed in ethanol: acetic acid (9:1, v/v) solution for 1–2 h, then transferred to 70% and 90% ethanol for washing. Seeds were then cleared in chloral hydrate solution, visualized by DIC microscopy in Zeiss Meta 510 confocal microscope.

Tetrazolium staining

Seed coat integrity was assessed by permeability test by incubating seeds in 1% 2, 3, 5-triphenyl tetrazolium chloride (Sigma) prepared in 50 mM phosphate buffer (pH 7.0) overnight at 30°C. After that image was captured with a stereomicroscope (Leica Microsystems) and quantification of red-pigmented seeds was performed. The experiment was performed in five replicates containing 50 seeds of different genotypes. In addition, a two-tailed Student's *t*-test was performed to check the significance.

Complementation line in the mutant *rabc1*-background

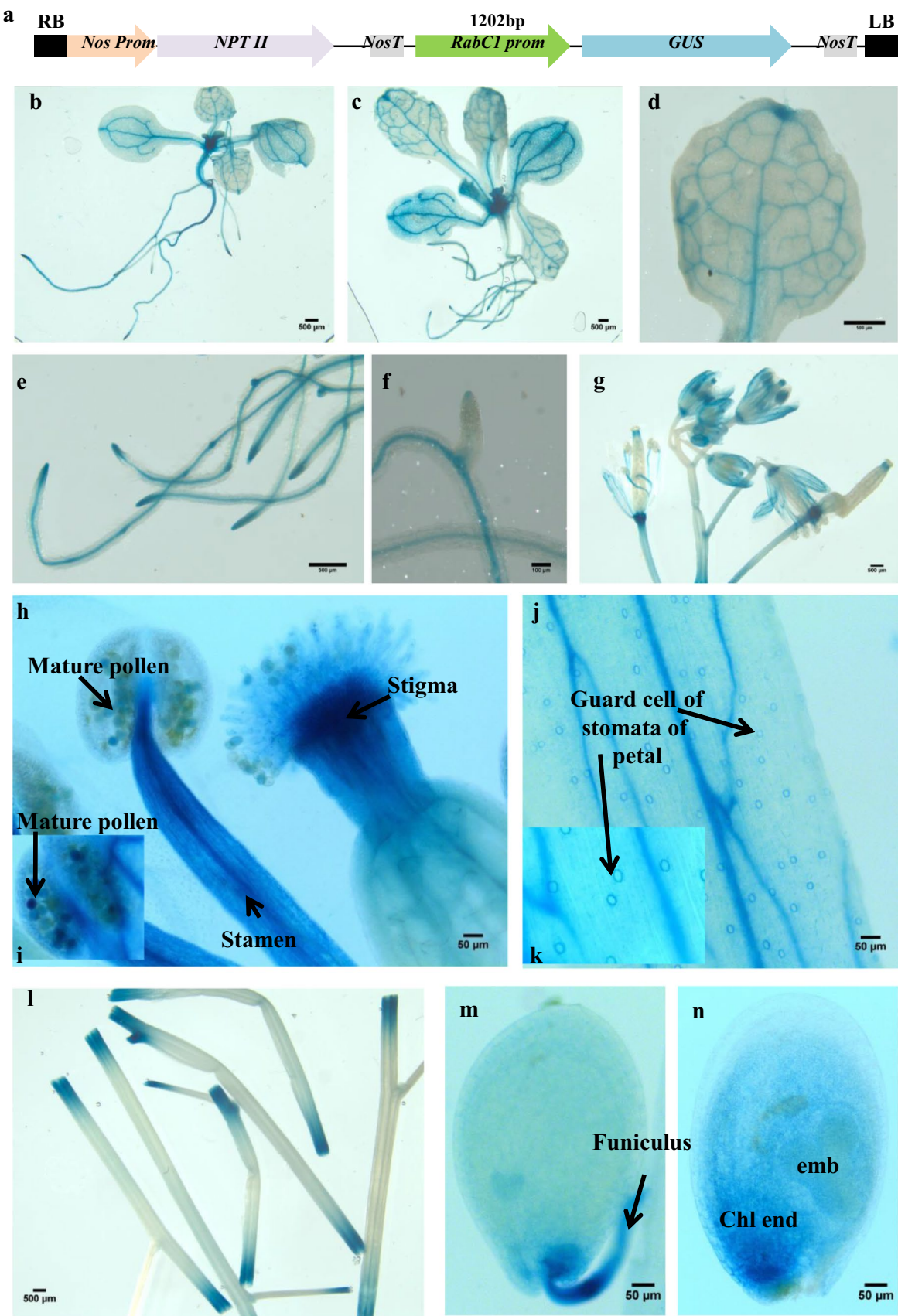
The complementation lines were developed in the mutant background, and a construct was prepared in the modified pBI121 having SmaI site at the 3' end of the *GUS* gene. In brief, the coding sequence of 639 bp having BamHI and SmaI sites was sub-cloned in pBluescript SK(+), and the clones were confirmed by Sanger sequencing. Digested promoters having HindIII and BamHI together with a digested fragment of coding sequences from Bluescript SK were triply ligated in HindIII, and SmaI digested pBI121 vector (without *GUS* gene). The positive construct was further confirmed by digestion with restriction enzyme HindIII (cf. Supplementary Fig. S8a, and b). The construct was transformed in *Agrobacterium*, followed by the transformation in *Arabidopsis* using the floral dipping method. Restoration of *RabC1* expression in transgenic lines in the mutant background was confirmed by qRT-PCR. The complementation line having the wild-type equivalent expression of *RabC1* in the mutant background was further selected for phenotypic analysis.

Staining of seed mucilage

Dry seeds were stained per the described protocol (Willats et al. 2001; Harpaz-Saad et al. 2011). Briefly, seeds were imbibed in water for 30–90 min and then stained with dye. For the visualization of acidic pectin, pre-hydrated seeds were stained with 0.01% ruthenium red (Sigma) with shaking for 20–30 min. Next, the cellulose and β-glucans were visualized by staining seeds with calcofluor white (Sigma) at a concentration of 25 µg/ml for 10 min. Stained seeds were washed multiple times and then visualized in the Leica fluorescence microscope under UV light.

Statistics

Biological replicates, sample size, and significance level were mentioned in all the figures, figure legends, and



◀Fig. 2 Tissue-specific expression of *RabC1* in different tissues. **a** Schematic representation of *RabC1_{prom}::GUS* construct. **b** GUS staining in a ten-day-old seedling. **c** A 15-day-old seedling. **d** Enlarged view of 15-day-old leaf. **e** Enlarged view of primary and secondary roots of 15-day-old seedling. **f** GUS staining at the tip of the secondary lateral root. **g** Inflorescence, bud, flower, and early stage of siliques. **h** Anther, stamen, and stigma. **i** An enlarged view of the anther. **j, k** Accumulation of GUS in guard cells and veins of petals. **l** Sections of cutted stem. **m** 4 DAP seed with funiculus. **n** 7 DAP seed. The experiment was performed in seven lines

supplemental data. Two-tailed *t*-tests and ANOVA have been performed in excel and GraphPad Prism 8.4.2 software.

Accession numbers

The accession numbers of genes specified in this study are as follows: AT1G43890 (*RabC1*), AT1G09380 (*UMAMIT25*), AT1G25270 (*UMAMIT24*), AT5G24910 (*CYP714A1*), AT2G26760 (*CYCB1-4*), AT3G48740 (*SWEET11*), AT5G13170 (*SWEET15*), AT4G05320 (*UBI10*), AT5G03530 (*RabC2A*), AT3G09910 (*RabC2B*).

Results

Identification and expression profiling of *Arabidopsis RabC1*

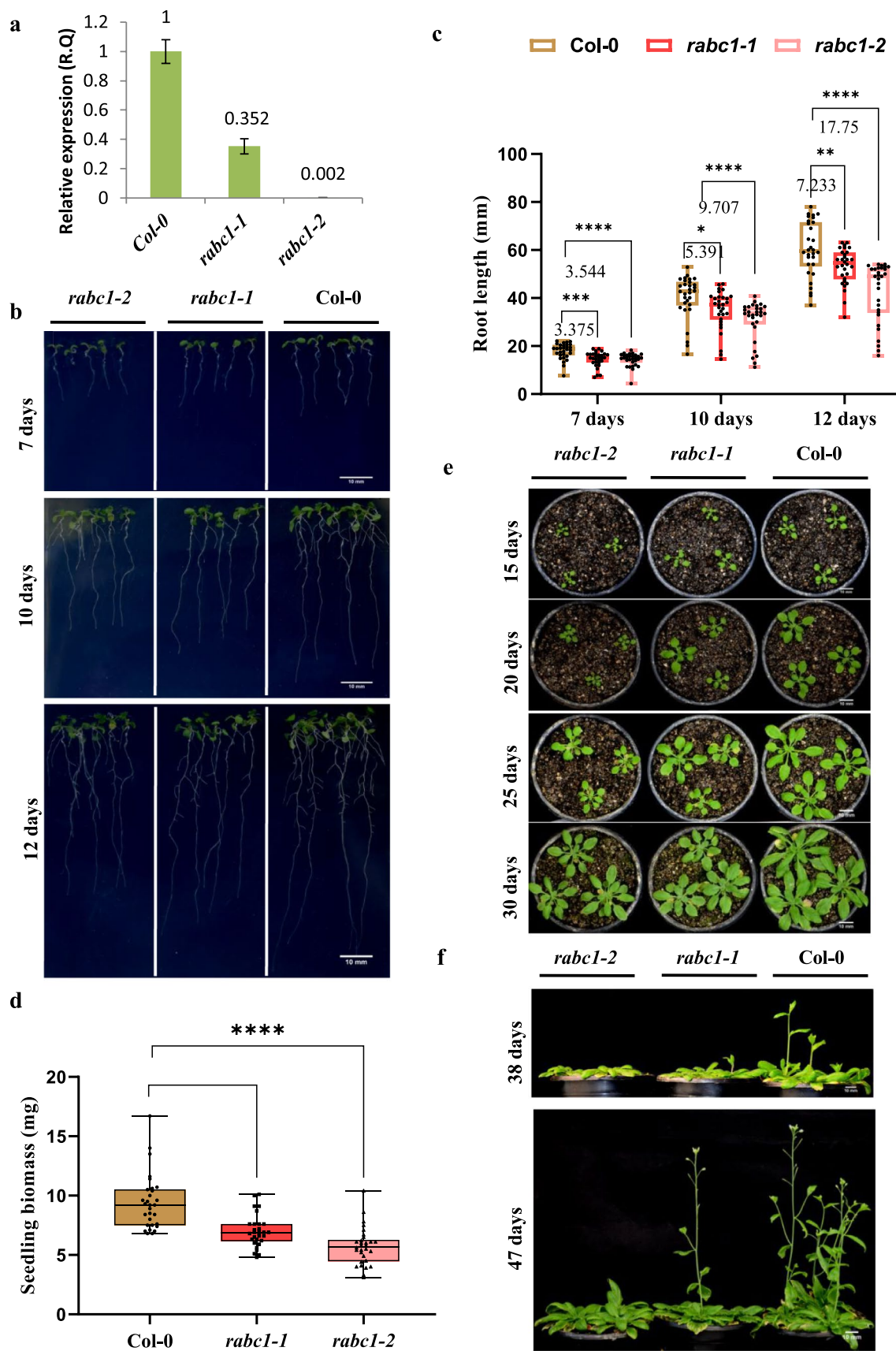
The *in silico* gene expression of 57 identified *Arabidopsis* Rab GTPases was performed in different plant developmental stages using Genevestigator to identify candidate GTPase with seed preferential expression. The developmental expression analysis revealed that most Rab GTPases were expressed differentially in various tissues (Supplementary Fig. S1). However, *RabC1*, *RabB1a*, and *RabH1a* have the highest expression in the chalazal endosperm stage (Supplementary Fig. S1). Furthermore, the expression of *RabC1* was significantly higher than *RabB1a* and *RabH1a* (Supplementary Fig. S2). It is also noteworthy that the expression of *RabC1* was elevated considerably in the seed-developing stages comprising chalazal endosperm, chalazal seed coat, and micropylar endosperm (Supplementary Fig. S1). Earlier studies suggested that chalazal endosperm mediates the delivery of nutrients between the maternal parent and growing embryo (Nguyen et al. 2000). Thus, we speculated that *RabC1* might have a role in cellular processes affecting the seed size and seed development.

RabC1 transcript variants and dynamics in their expression pattern along the developmental stages

The expression of *RabC1* transcript was assessed using qRT-PCR in three stages of developing seeds in *Arabidopsis* viz.,

early seed development stages at 3, 4, 5, and 6 DAP siliques; maturation stage at 8, 10, and 12 DAP; and late maturation stages at 16 DAP and also in other tissues (Fig. 1a, and b; primers indicated by orange color arrows, Fig. 1c). First, the transcript level of *RabC1* was highest at 3 DAP siliques; then it fell sharply at 4 DAP siliques. Further, it gradually increased up to 6 DAP siliques and decreased again at 8 DAP and then steadily increased afterward until the late phase (Fig. 1a). The expression pattern of the *RabC1* transcript was elevated at three developmental stages, i.e., the early coenocyte phase of endosperm (3 DAP); endosperm cellularization stage (6 DAP) which is important for the final seed size (Zhang et al. 2020) together with seed filling during seed maturation and late maturation (16 DAP) stage (Fig. 1a). We also analyzed transcript levels in various vegetative tissues: leaf, rosette, stem, flower, bud, and root, and the expression was found to be highest at the bud stage, followed by root, flower, stem, rosette, and least at the mature leaf (Fig. 1b).

The *RabC1* gene consists of three transcript isoforms viz., *RabC1.1*, *RabC1.2*, and *RabC1.3* that translate to identical proteins (Fig. 1c). The transcription start sites (TSS) of each isoform seem to be at a different position (Fig. 1c). These isoforms have differences in 3' and 5' UTR sequences (Supplementary Fig. S3). Considering the differences, at the 5' UTR of *RabC1.3*, there was intron retention (Fig. 1c indicated by 'x') which appears to be spliced out in the mature mRNA of *RabC1.1* and *RabC1.2* isoforms. The occurrence of intron retention might be due to the TSS switching for the generation of different splice variants. Furthermore, 3' UTR of isoform *RabC1.1* and *RabC1.3* was similar except for the addition of 22 nucleotides at the end of 3' UTR of *RabC1.1*. However, *RabC1.2* poses a relatively shorter 3' UTR due to some portion spliced out (Fig. 1c indicated by 'y') in the form of an intron in the mature mRNA, and besides this, it also contains six extra adenine at the 3' UTR (Fig. 1c indicated by 'z'). We thus assessed the expression level of these variants using isoform-specific primers in the qRT-PCR analysis (Fig. 1d, Supplementary Fig. S3a and b). We examined the isoform-specific expression (Fig. 1c primers denoted by arrows with different colors and S3a) in multiple tissues: leaf, rosette, stem, flower, bud, root, and three developing seed stages; 3, 5, and 16 DAP siliques. The expression of the variants *RabC1.1* and *RabC1.3* was lower in all tissues investigated than the cumulative expression of *RabC1*, which demonstrated a high level of expression (Fig. 1d). The *RabC1.2* primers cannot differentiate these isoforms; thus, the expression of *RabC1.2* was higher (app. 75–80%) among all the variants but not equal to the cumulative expression of *RabC1* (Supplementary Fig. S3a, and b). The isoform *RabC1.3* showed relatively higher expression in roots compared to other tissues; while *RabC1.2* or *RabC1* was expressed predominantly in the 3 DAP stages of siliques



◀Fig. 3 Phenotypic characterization of *RabC1*. **a** Relative expression of *RabC1* transcript in Col-0, *rabc1-1*, *rabc1-2*. Transcript level was checked by qRT-PCR from primers designed downstream of T-DNA insertion. A total of two biological replicates in *Arabidopsis* Col-0, five in *rabc1-1*, two in *rabc1-2*, and each with two technical replicates was taken. Standard bars represent SE. **b** Comparative growth analysis of seven-day-old, ten-day-old, and 12-day-old Col-0, *rabc1-1*, and *rabc1-2* seedlings. The image is representative of six biological replicates. Each plate contains five seedlings of all three genotypes, Col-0, *rabc1-1*, and *rabc1-2*. **c** Quantitative analysis of root length of seven-day-old, ten-day-old, and 12-day-old Col-0, *rabc1-1*, and *rabc1-2* seedlings. Box plots are represented by median (lines), interquartile ranges (boxes), and whiskers of root length of various genotypes (Col-0, *rabc1-1*, and *rabc1-2*; $n=30$). Each dot represents the sample. **d** Biomass determination of 12-day-old Col-0, *rabc1-1*, and *rabc1-2* seedlings. Box plots showing median (lines), interquartile ranges (boxes), and whiskers of seedling biomass of the genotypes as mentioned above. **e** Morphological analysis of 15-day-old, 20-day-old, 25-day-old, and 30-day-old Col-0, *rabc1-1*, *rabc1-2* plants. Scale bar = 10 mm. **f** Comparison of flowering time of 38-day-old and 47-day-old Col-0, *rabc1-1*, *rabc1-2* plants. The image is representative of three independent replicates. Seedling experiments were performed three times and showed consistent results. Scale bar = 10 mm. Significance denoted by asterisks * at $P < 0.05$, ** at $P < 0.01$, *** at $P < 0.001$, and **** at $P < 0.0001$

development (Fig. 1d). Apart from *RabC1*, the *RabC* family contains two other members, *RabC2A* and *RabC2B*. All three *RabC* proteins show a high degree of homology among their isoforms (Hashimoto et al. 2008). However, the transcript abundance of *RabC2A* and *RabC2B* in different tissues reveals its preferential expression in the root and stem in contrast to *RabC1*, which showed their highest expression in siliques (Supplementary Fig. S4a, and b; and Fig. 1a, and d).

Tissue-specific expression of *RabC1* and the analysis of cis-regulatory motifs in the promoter region

The spatiotemporal expression of *RabC1* was further investigated by fusing 1202 bp promoter sequence (Supplementary Fig. S5a), including 5' UTR from upstream of the ATG to *GUS* reporter gene (Fig. 2a, and Supplementary Fig. S5a) as previous studies in *Arabidopsis* suggests that 500 bp-1kb is sufficient to emulate transcription behavior of a promoter (Maston et al. 2006; Srivastava et al. 2014; Mishra et al. 2022; Prasad et al. 2022). The promoter construct was stably transformed in *Arabidopsis*, and several independent lines were analyzed for GUS expression using histochemical staining. In the vegetative development stage, GUS staining was observed in the shoot and roots of 10-day-old seedlings, and expression was more prominent in the leaf veins and nodes (Fig. 2b). We also observed GUS staining in the primary and secondary roots (Fig. 2b, c, e, and f). In 15-day-old seedlings, expression was persistent in the shoot, roots, leaf veins, nodes, and the leaf tip (Fig. 2c, and d). We also found a strong expression at the primary and secondary root tips (Fig. 2e and f). In the reproductive stage, strong

GUS expression was observed in the petal, the base of the flower (Fig. 2g), the stamen, the anther, mature pollen, and the stigma (Fig. 2h and i). We also detected prominent staining in the petals' guard cells and veins (Fig. 2j and k). GUS expression was also apparently strong at the cut part of the stem (Fig. 2l).

In the developing seed, maximum GUS expression was observed at the chalazal endosperm, followed by the chalazal seed coat. A low but distinct expression was also seen in the embryo (Fig. 2m and n). Interestingly, intense GUS staining was also observed in the funiculus tissue (Fig. 2m) that connects the developing seeds to the maternal parent and is known to be responsible for the direct transport of nutrients and the developmental signal from maternal tissues to seeds (Khan et al. 2015). Thus, it can be concluded that *RabC1* is widely expressed in all organs, with its maximum expression in the chalazal endosperm suggesting its role during seed development.

The *in-silico* promoter analysis using PlantCARE (Lescot et al. 2002) and PLACE (Higo et al. 1999) indicated several *cis*-regulatory elements involved in plant development, hormonal regulation, and stress response in the promoter of *RabC1* (Supplementary Fig. S5b). Further, light responsiveness motifs that include ACE, G-box, GT1-motif, and P_c-CMA2a were also enriched in the promoter regulatory region. The endosperm-specific skn-1 motif (Supplementary Fig. S5b) correlated with *RabC1*'s maximum expression in seed (Fig. 1a and 2n), suggesting its role in seed development. A significant number of GA responsive elements (GARE-motif and TATC-box) were located at various positions (+ 242, + 893, + 414, and - 93) and predicted to be involved in plant signaling. *RabC1* promoter also harbors two TCA elements required for salicylic acid responsiveness at positions + 396 and - 1056. Different *cis*-regulatory elements were identified as associated with abiotic stress responses that included ABRE, DRE, HSE, and MBS were also present in the *RabC1* promoter (Supplementary Fig. S5b).

The high number of gibberellin responsive (Four, GARE-motif, and TATC-box) and SA-responsive elements (two TCA elements) in the *RabC1* promoter indicates its responsiveness towards these phytohormones. We thus subjected *RabC1* promoter-GUS fusion lines to 200 μM GA3 and 2 mM SA treatment. The histochemical and quantitative enzyme activity assay showed that the *RabC1* promoter does not respond to GA3 despite having a significant number of conserved GA-responsive elements (Supplementary Fig. S6). However, we identified intense histochemical GUS staining and elevated but insignificant quantitative GUS activity increase in response to SA compared to control (Supplementary Fig. S6a, and b).

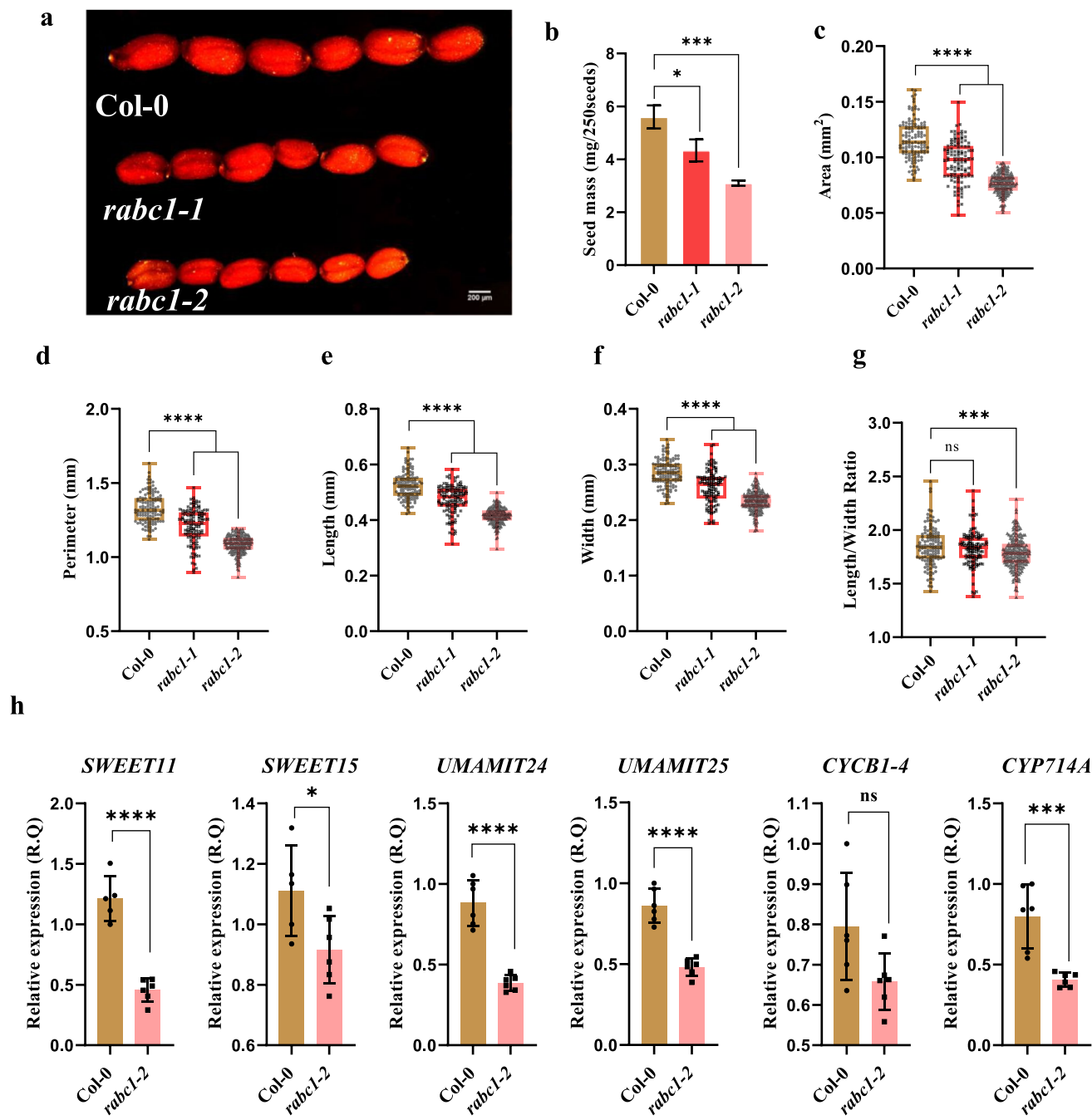


Fig. 4 Differences in the seed phenotype of Col-0, *rabc1-1*, and *rabc1-2*. **a** Seed size of different genotypes (Col-0, *rabc1-1*, *rabc1-2*). Scale bar = 200 μ m. **b** Determination of seed mass of 250 seeds of each Col-0, *rabc1-1*, and *rabc1-2* in five biological replicates. Error bars denote standard deviation (SD). **c–g** Quantitative analysis of seed parameters in Col-0, *rabc1-1*, and *rabc1-2*. **c** Area. **d** Perimeter. **e** Length. **f** Width. **g** Length/width ratio (Col-0, $n=128$; *rabc1-1*, $n=110$; *rabc1-2*, $n=225$). Box plots indicate the median (lines), interquartile ranges (boxes), and whiskers of the above seed size variables, area, perimeter, length, and width. Each point represents the

sample. The experiment was repeated two times with similar results. **h** Validation of seed phenotypes by expression analysis of sugar transporters genes, *SWEET11*, and *SWEET15*, amino acid transporters *UMAMIT24*, and *UMAMIT25*, *CYCB1-4*, and *CYP714A* in 5DAP seeds of *rabc1-2* and Col-0. The experiment was executed in six replicates with two biological and three technical replicates. Error bars denote the standard deviation (SD) among replicates. Significance denoted by * at $P < 0.05$; ** at $P < 0.01$; *** at $P < 0.001$; and **** at $P < 0.0001$

Mutation in *RabC1* affects plant growth, root length, and flowering time

RabC1 encodes a protein of 212 amino acids that belongs to the Rab family of small GTPases (Supplementary Fig. S7a). To demonstrate the role of *RabC1* in plant growth and development, we assessed the expression of *RabC1* in T-DNA insertional mutants. The qRT-PCR for the *RabC1* gene confirmed that the transcript level was reduced significantly to 35% compared to WT in *rabc1-1*, while in intronic mutant *rabc1-2*, no transcript was detected (Fig. 3a). Thus, *rabc1-1* is a knock-down mutant while *rabc1-2* is a knock-out mutant. We compared the seedling growth and root length in *rabc1-1* and *rabc1-2* with that of the wildtype (WT) Col-0 at seven-day-old, ten-day-old, and 12-day-old seedlings. It was apparent that the seedling growth and root length in *rabc1-1* and *rabc1-2* were compromised as compared to WT (Fig. 3b). The quantitative analysis of root length also indicated that root length was highly reduced in *rabc1-2* than in *rabc1-1*, with a significant difference of 7.233 mm in the case of *rabc1-1* and 17.75 mm in the case of *rabc1-2* at 12 days after germination (DAG) as compared to WT (Fig. 3c). However, seedling biomass was comparable in *rabc1-1* and *rabc1-2* to WT, with relatively lesser biomass in *rabc1-2* (Fig. 3d). The qualitative and quantitative analysis of root length strongly suggests that *rabc1-2* phenotype was more profound than *rabc1-1* (Fig. 3b, and c), which was highly correlated with the expression pattern of *RabC1* in mutant's *rabc1-1*, and *rabc1-2* (Fig. 3a). Collectively, these results suggest that *RabC1* is required for plant growth and root development.

To further gain insight into the importance of *RabC1* in the later stages of plant development, the *rabc1-1*, *rabc1-2*, and Col-0 phenotypic analyses were performed in multiple replicates before and after the flowering stages of plant development (Fig. 3e, and f). Before flowering stages, such as 15-day, 20-day, 25-day, and 30-day-old, plants of *rabc1-1* and *rabc1-2* exhibited comparatively dwarf phenotypes with less expanded leaves and smaller rosette size than WT (Fig. 3e). Later, we observed delayed flowering in *rabc1-1* and *rabc1-2* compared to WT (Fig. 3f). In the case of *rabc1-1*, we have seen a few replicates flowered normally which may be due to the knock-down expression of *RabC1*. However, in the case of *rabc1-2*, flowering was delayed comparatively which correlates with their complete loss of transcript because of their T-DNA insertion in the genic region (Fig. 3a, and f). Overall, these results highlight the crucial role of *RabC1* in cellular processes important for normal plant development.

RabC1 affects seed size and cell expansion during seed development

Our expression analysis implies that *RabC1* exhibited a maximum expression at early seed development; 3 DAP and 6 DAP and specifically at chalazal endosperm, chalazal seed coat, and funiculus that are essential tissue for the transport of nutrients to the developing embryo (Fig. 2m, 2n, and Supplementary Fig. S1). Thus, to define the role of *RabC1*, seeds collected from homozygous mutants *rabc1-1* and *rabc1-2* were examined. We observed a smaller seed size in the mutants of *RabC1* compared to WT, with *rabc1-2* exhibiting the smallest seed size compared to *rabc1-1* (Fig. 4a). Furthermore, seed weight was also significantly lesser in the *rabc1-1* and *rabc1-2* compared to WT (Fig. 4b). The quantitative analysis also revealed that seed area, perimeter, length, and width of *rabc1-1* and *rabc1-2* were significantly reduced compared to WT (Fig. 4c, d, e, and f). The length/width ratio of *rabc1-1* was similar to WT while *rabc1-2* showed a significantly reduced ratio (Fig. 4g). Together, these results suggest that mutation in the *RabC1* gene affects seed size. The knockout mutant displayed a more pronounced phenotype of reduced seed size and weight than the knock-down mutant.

Expression analysis was performed by taking previously reported marker genes to validate the seed phenotypes of mutants. We analyze the expression of genes implicated in seed size and seed filling in knockout mutant *rabc1-2* and WT at 5 DAP seeds. In Arabidopsis, developing embryos rely on the nutrition provided by the maternal tissues through the activity of various sugar transporters located in the seed coat and endosperm (Chen et al. 2012, 2015). We determined the expression of *SWEET11* and *SWEET15*, and we found that the expression of both genes was significantly downregulated in *rabc1-2* (Fig. 4h).

Furthermore, several reports suggest that numerous UMAMIT proteins are expressed in the developing seeds during the seed-filling process, participate in the transport of amino acids, and contribute to the seed yield (Mu et al. 2015; Besnard et al. 2018). We found that the expression of *UMAMIT24* and *UMAMIT25* was affected and significantly downregulated in *rabc1-2* (Fig. 4h). We also analyze the expression of some known seed size regulators reported previously to validate the seed phenotypes (Ren et al. 2019). In Arabidopsis, *CYCB1; 4*, a positive seed size regulator. We found its expression was downregulated in *rabc1-2* (Fig. 4h). Further, Arabidopsis *CYP714A1* or *ELA1* encodes a cytochrome p450 monooxygenase which is a negative seed size regulator that deactivates the bioactive GAs, thus affecting cell wall expansion (Zhang et al. 2011; Creff et al. 2015). We analyzed the transcript abundance of *ELA1*, which was also downregulated (Fig. 4h). Collectively, the above results point toward the role of *RabC1* during seed development

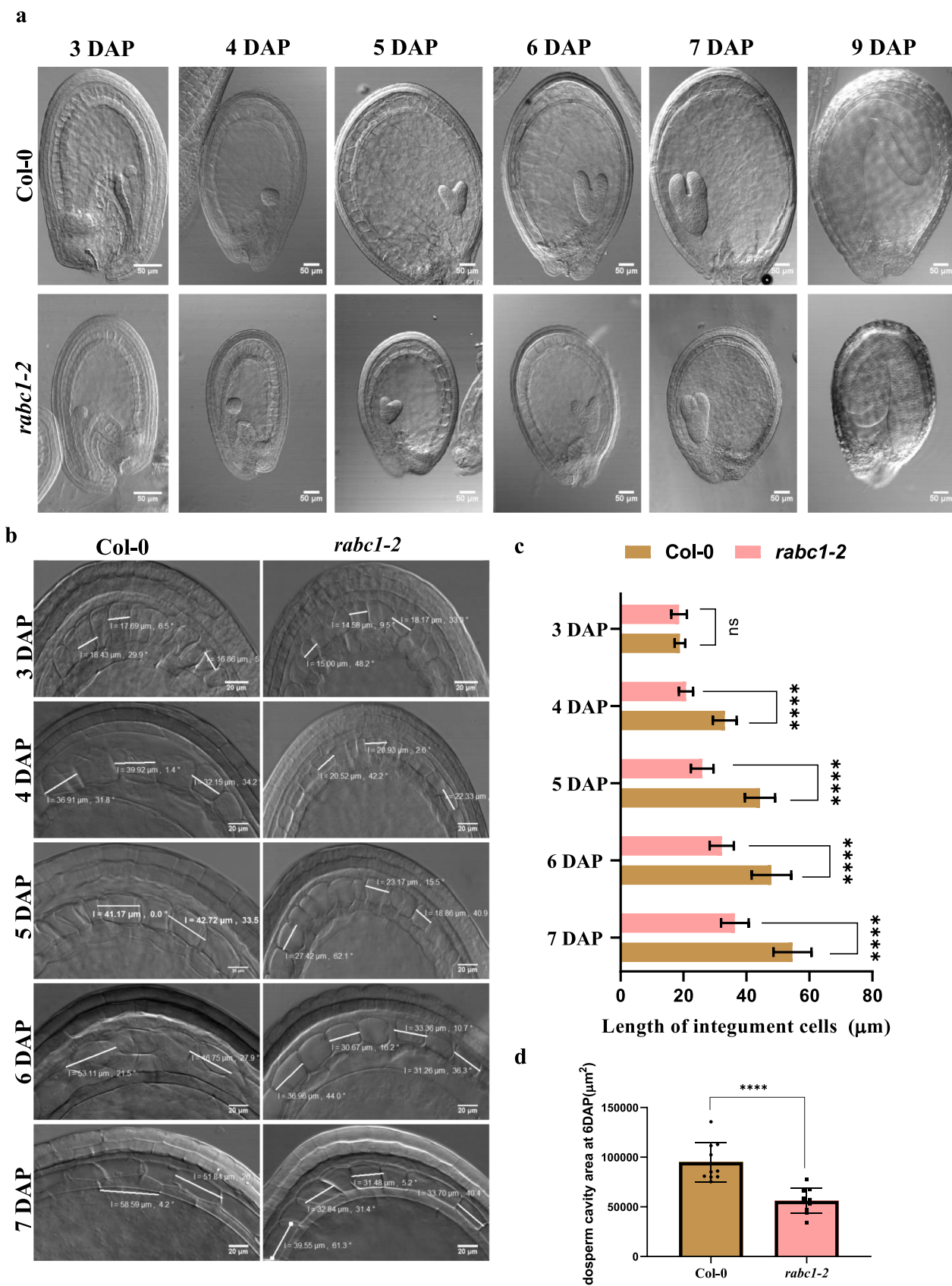


Fig. 5 RabC1 is required for cell expansion during seed development. **a** Differential interference contrast microscopy (DIC) of randomly selected seeds at various stages of seed development (3DAP, 4DAP, 5DAP, 6DAP, 7DAP, and 9DAP) in WT and *rabc1-2*. Scale bars = 50 μ m. **b** Microscopical image of an enlarged view of integument cells of different genotypes, WT and *rabc1-2* in several seed developing stages (3DAP–7DAP). Scale bars indicate 20 μ m. **c** Quantitative measurement of the length of integument cells in genotypes, WT, and *rabc1-2*, at numerous stages of seed development 3DAP to 7DAP (WT at 3–7DAP, $n=30, 25, 19, 14, 13$; and *rabc1-2* at 3DAP to 7 DAP, $n=20, 18, 16, 23, 17$). **d** Comparative analysis of endosperm cavity area of WT and *rabc1-2* at 6DAP stage (WT and *rabc1-2*, $n=10$). The experiment was performed two times and showed similar results. Asterisks represent significance level (two-tailed *t*-test), where * at $P<0.05$, ** at $P<0.01$, *** at $P<0.001$, and **** at $P<0.0001$

and is positively implicated in the seed-filling process by an unknown mechanism.

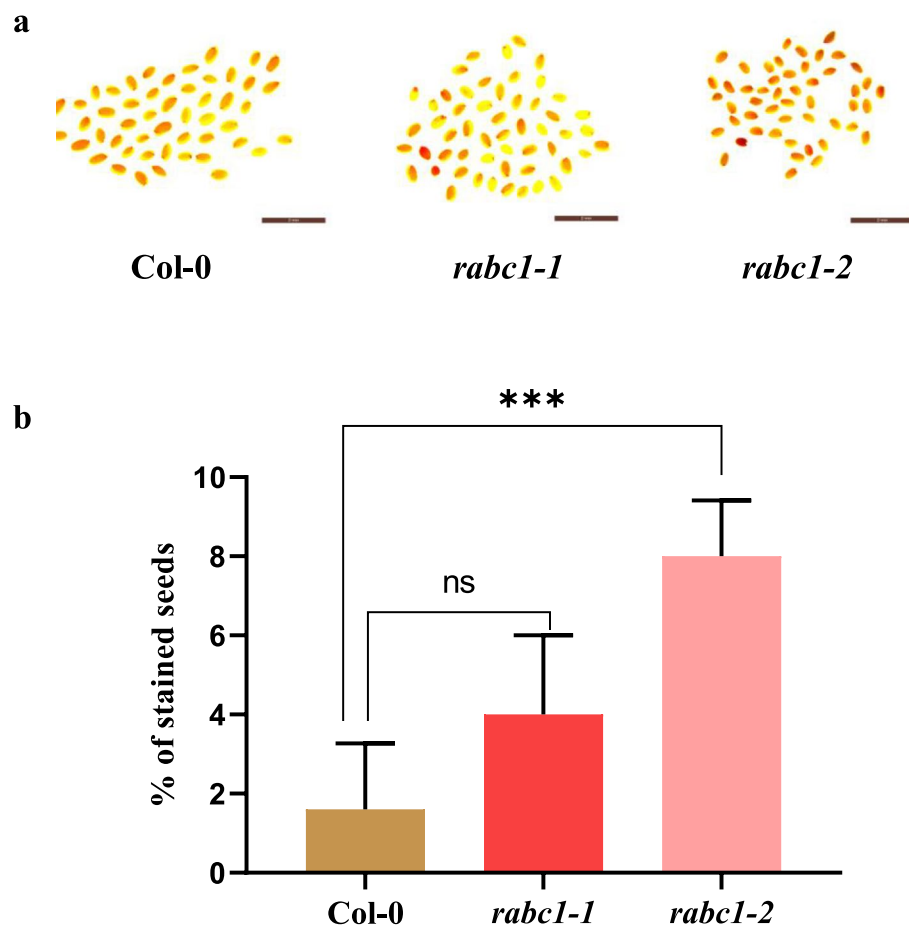
To further gain insight into the details of the internal structure of developing seeds, differential interference contrast (DIC) microscopy was performed at various stages of seed development, comprising 3, 4, 5, 6, 7, and 9 DAP. The cytological study revealed that embryo development in *rabc1-2* was proper and similar to WT in all stages of

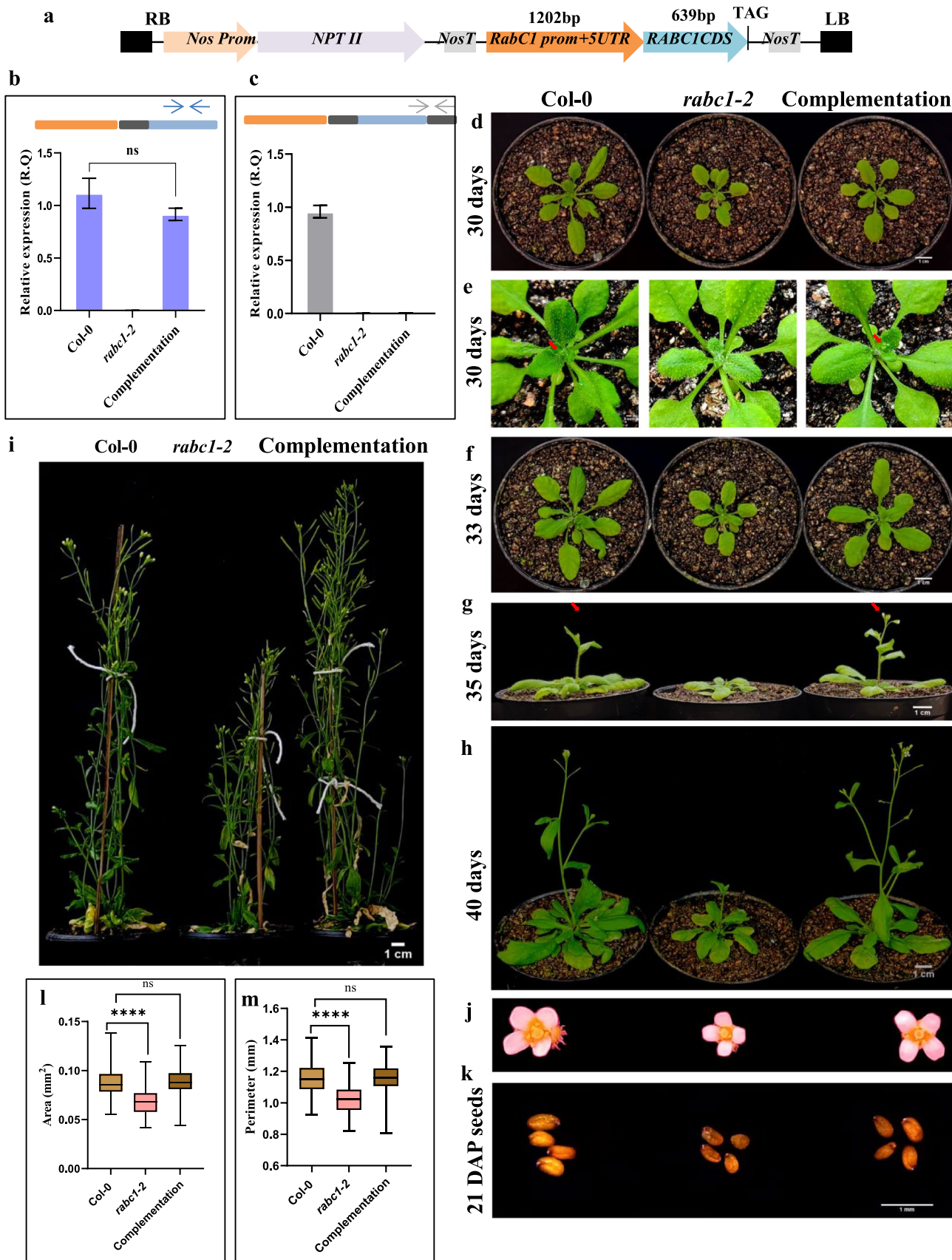
developing seeds (Fig. 5a). We found a reduced expansion of the endosperm cavity from 4 to 7 DAP in *rabc1-2* compared to WT (Fig. 5a). At 3 DAP, cell integument length was almost similar in *rabc1-2* and WT (Fig. 5b, and c). Beyond 3 DAP, we observed less cell expansion in the integument from 4 to 7 DAP of developing seeds (Fig. 5b). The quantitative analysis of cell integument length from 3 to 7 DAP stages also indicated that *rabc1-2* showed significantly decreased cell integument length than WT (Fig. 5c). Since at 6 DAP the endosperm cavity almost attains its full size, which determines the final seed size, we performed a quantitative analysis of the endosperm cavity area in *rabc1-2* with WT. Notably, we found a significantly smaller area of the endosperm cavity in *rabc1-2* compared to WT (Fig. 5d). The cumulative results suggest that RabC1 GTPase contributes to cellular processes required for the expansion of the endosperm cavity and integument cells.

Mutation in *RabC1* affects seed coat permeability

The RabC1 was hypothesized to play role in nutrient transport and seed coat permeability because of high expression in the chalazal seed coat and funiculus (Fig. 2m, and n).

Fig. 6 Mutation in *RabC1* affects seed coat permeability. **a** Seeds of WT, *rabc1-1*, and *rabc1-2* after overnight incubation in tetrazolium chloride dye. **b** Quantitative analysis of stained seeds of WT, *rabc1-1*, and *rabc1-2* in five biological replicates, each containing 50 seeds. Asterisks indicate * as a significant difference between mutants and WT (two-tailed *t*-test). * at $P<0.05$, ** at $P<0.01$, *** at $P<0.001$, and **** at $P<0.0001$





◀Fig. 7 Restoration of phenotypes in the complementation line generated in *rabc1-2*. **a** Schematic representation of *RabC1_{prom}::CDS* restorer construct. **b** Relative expression of *RabC1* in Col-0, *rabc1-2*, and complementation line. Arrows represent the position of the primers, and error bars indicate the standard deviation. **c** Relative expression of *RabC1* of WT specific allele in the Col-0, *rabc1-2*, and complementation line for confirming mutant background. Arrows represent the position of the primers (orange, blue, and grey bars indicate the promoter, coding sequence, 3' and 5' UTR). **d** Phenotype of Col-0, *rabc1-2*, and complementation line at 30DAG. **e** Zoom image showing initiation of flowering in Col-0, complementation line in contrast to *rabc1-2*. **f, g, h**, and **i** Morphological analysis of Col-0, *rabc1-2*, and complementation line in 33-day-old, 35-day, 40-day-old and mature plants. **j** Comparison of flower phenotype in Col-0, *rabc1-2*, and complementation line. **k** Seed phenotype of Col-0, *rabc1-2*, and complementation line at 21 DAP stage. **l, m** Comparison of area and perimeter of Col-0, *rabc1-2*, and complementation line seeds ($n=174, 120$, and 160)

The seed coat permeability was assessed by staining seeds with tetrazolium chloride, a colorless dye. Upon exposure to enzymes of live tissue, it gets reduced to red formazan. We observed a significantly higher number of stained seeds in the knockout mutant *rabc1-2* compared to WT (Fig. 6a, and b). On the other hand, there was no significant difference in the knock-down mutant *rabc1-1* compared to WT (Fig. 6b). These results indicate that the lack of function of RabC1 increases the permeability of the seed, which may be due to defects in the seed coat integrity.

Functional complementation in the *rabc1-2* mutant

Complementation lines were generated in the knock-out *rabc1-2* mutant background (Supplementary Fig. S8). The complementation lines with a functional copy of RabC1 driven by the native promoter showed RabC1 transcript abundance comparable to that of the WT in the quantitative RT-PCR analysis (Fig. 7a, Supplementary Fig. S8 and S9). The complementation line in which the expression of RabC1 was equivalent to WT was subjected to phenotypic analysis (Fig. 7b, c and Supplementary Fig. S8 and S9). The detailed phenotypic study at 30, 33, 35, and 40 DAG, showed that the rosette diameter, flowering time, flower size, bolting, and plant height of the complementation line were similar to that of the WT (Fig. 7d–j). In addition, we also observed the restoration of seed development defects in 21 DAP siliques of the complemented line, with an average seed size comparable to that of the WT (Fig. 7k, l, and m).

The correlation of gene expression among the three members of the RabC family was also assessed. The transcripts level of *RabC2A* was similar in the Col-0, *rabc1-2*, and complemented lines, implying no compensation at the transcript level (Supplementary Fig. S10a). In contrast, the transcript level of *RabC2B* was reduced in *rabc1-2* as compared to Col-0, and it got partially restored in the complemented lines (Supplementary Fig. S10b), suggesting that there is

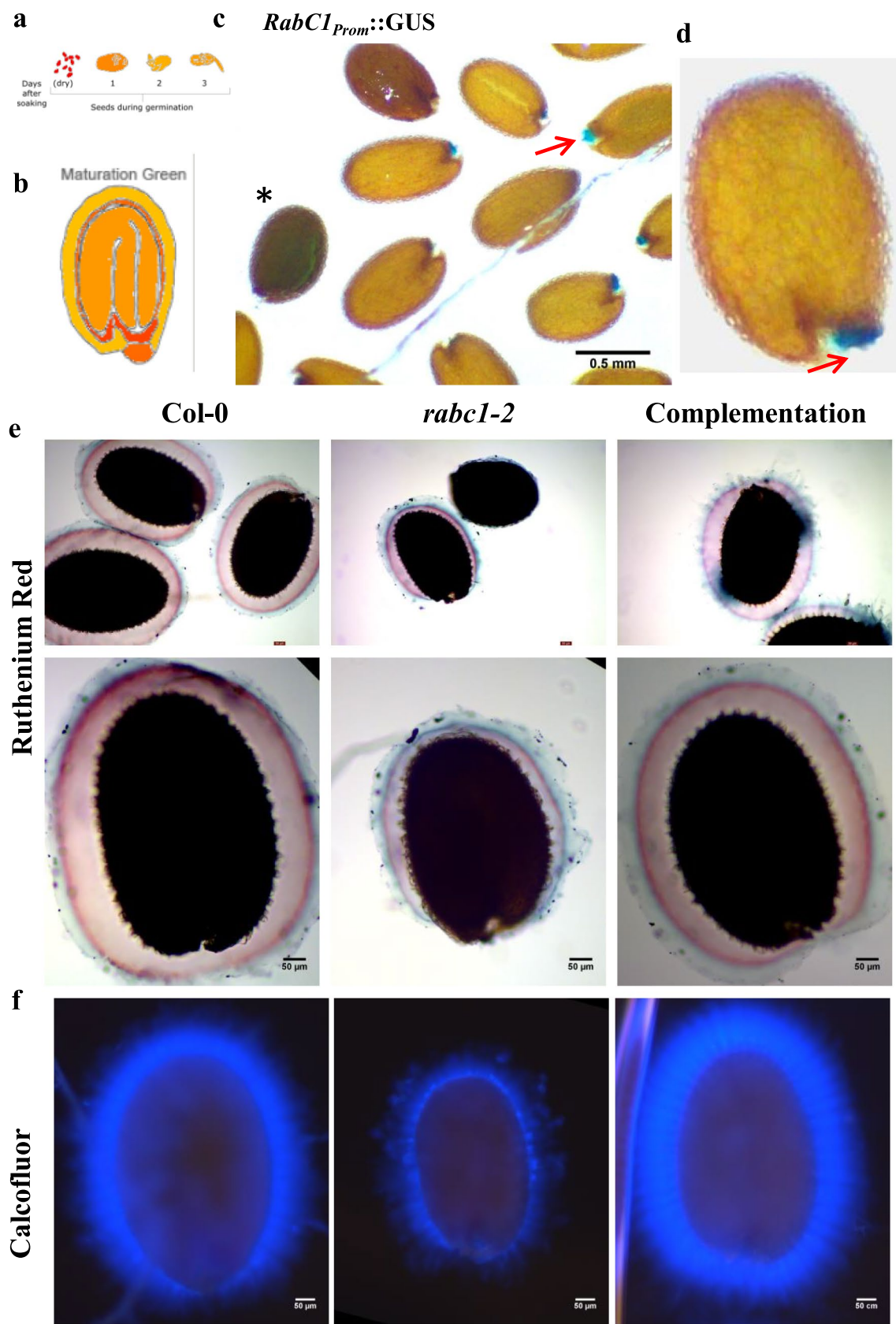
some unknown mechanism that correlates the expression of *RabC1* and *RabC2B*. However, the elevated expression level of *RabC2B* in the complemented lines was not similar to the WT level that might be due to some experimental variation. Overall, the complementation experiment showed that RabC1 with its native promoter could rescue plant growth and seed defects of the mutant supporting functional complementation.

RabC1 is required for seed mucilage formation

The *in-silico* expression using the eFP browser (Winter et al. 2007) showed the expression of *RabC1* in the green maturation seed stage and the dry seed (Fig. 8a and b). We also observed GUS expression in the ruptured dry seed beneath the brown seed coat (Fig. 8c, denoted by an asterisk) and the chalazal seed coat region in the GUS-promoter reporter lines (Fig. 8c, and d). Thus, the expression of *RabC1* in the different seed tissues prompted us to analyze the status of seed mucilage in *rabc1-2*. First, we stained the seeds with ruthenium red to examine the seed mucilage in the WT and *rabc1-2*. The *rabc1-2* mutants showed reduced seed mucilage staining compared to WT. However, the seed mucilage staining was comparable to WT in the complemented line, indicating that the mucilage defects were rescued (Fig. 8e). To examine cellulose, which is the critical constituent of seed mucilage, we stained the seeds with calcofluor white. The WT seeds showed broad, intense fluorescence, while the fluorescence was reduced in *rabc1-2*. However, in the complemented line, we observed fluorescence similar to WT suggesting the involvement of *RabC1* in the trafficking of mucilage components during seed mucilage synthesis and deposition (Fig. 8f).

Discussion

Angiosperms are the most dominant life form of the plant due to their ability to develop seeds that house the next generation. Seeds germinate and revive into the fully grown plant on receiving appropriate conditions. Plant growth and development need numerous signaling pathways to be activated precisely temporally and spatially by key regulators. Rab GTPases are key regulators that mediate the transport of molecules to their respective compartments according to the demand (Olkkinen and Slenmark 1997; Pereira-Leal and Seabra 2001; Nielsen 2020). Several Rab GTPases have been reported to localize to distinct compartments. The localization of RabC1 is uncharacterized (Wang et al. 2022). Few reports predict its localization to post Golgi/endosome, but its functional characterization has not yet been done (Rutherford and Moore 2002; Zhou et al. 2020).



◀Fig. 8 RabC1 is required for seed mucilage. **a** Expression of *RabC1* in the dry seed via eFP browser. **b** At the maturation green stage. **c** GUS expression in the dry seed. **d** Enlarged image showing GUS expression at the chalazal seed coat region in the *RabC1_{prom}::GUS* reporter line. The mature, dry seeds were kept in GUS solution overnight and then visualized under a microscope. **e** Ruthenium red staining in the pre-hydrated seeds of Col-0, *rabc1-2*, and complementation line. **f** Calcofluor white staining in the pre-hydrated seeds of Col-0, *rabc1-2*, and complementation line. The experiment was performed two times with similar results

Among the three Rab GTPases preferentially expressed in seed tissue, *RabC1* showed the highest expression level, indicating its substantial role in the seed (Supplementary Fig. S1, and S2). Besides, among the three members of the RabC family, *RabC1* shows the highest expression (Fig. 1a, b, d, and Supplementary Fig. S3). The expression of *RabC1* in different stages of the plant development also suggests its involvement in various processes (Fig. 1a, b, Supplementary Fig. S1 and S2). Furthermore, its pattern of expression during different developing stages of seed also reveals that it is involved in the three transition stages; early seed development, endosperm cellularization, and seed maturation (Fig. 1a, and b).

Several reports indicate that housekeeping genes harbor a single UTR and are expressed constitutively in numerous processes (Eisenberg and Levanon 2003). Some studies also emphasize that most of the ubiquitously transcribed genes produce various 3' UTRs through tissue-specific alternative polyadenylation to gain specificity. The 3' UTR isoform ratios appear to be cell type-specific and crucial for particular pathways (Kesari et al. 2012; Lianoglou et al. 2013; Zheng 2018). We found that *RabC1* consists of three isoforms that produce identical proteins. These isoforms have differences in their 5' UTRs and 3' UTRs (Fig. 1c, Supplementary Fig. S3a).

Furthermore, isoform-specific expression analysis in different stages of plant development and developing seeds indicates their expression pattern and level dynamics (Fig. 1d). A comparative analysis of the expression level of isoforms showed that *RabC1.2* showed the highest transcript abundance at 3 DAP siliques (Fig. 1d). Several findings reveal that shorter 3' UTR have more regulatory functions, as lengthy 3' UTR occlusive topologies make regulatory components less accessible (Lianoglou et al. 2013). Furthermore, these 3' UTR have relatively short UTR due to using the closest polyadenylation (pA) site (Kim et al. 2014; Mayr 2017). Interestingly, the *RabC1.2* isoform has a shorter 3' UTR (Fig. 1c, and Supplementary Fig. S3a) and exhibits high expression, too (Fig. 1d). With the help of publicly available tools (Weigel and Mott 2009), we found that *RabC1.2* genomic locus carried single nucleotide polymorphism (SNPs) towards 3' end of the gene in 10 natural ecotypes (Supplementary Table S2). The particular SNPs

are categorized under splice acceptor variant, and their effect is considered high, indicating their importance towards the 3' end of the gene (Supplementary Table S2). The above findings suggest that abundantly expressed *RabC1* likely controls tissue-specific functions through the generation of isoform under the tight regulation by 3' UTR.

Spatiotemporal expression using the GUS promoter line further confirmed the tissue-specific localization of *RabC1* (Fig. 2). We observed GUS staining in almost all tissue: seedling, root, secondary lateral root, leaf, leaf tip, veins, and reproductive tissues, suggesting *RabC1*'s role in all aspects of development (Fig. 2b, c, d, e, f, and g). GUS staining at the cut part of stems further indicates its involvement in wound responsiveness (Fig. 2l). Specific expression in the guard cell of flower petals documents its role in stomatal biology (Fig. 2j, and k). During seed development, GUS staining was found to accumulate at the chalazal endosperm, embryo, and funiculus, which was strong evidence of its role in seed development and seed size (Fig. 2m, and n). Overall, expression analysis prompted us further to characterize the role of *RabC1* in plant development.

To further characterize the phenotype of *RabC1*, a comparative study was performed on *rabc1-1*, *rabc1-2*, and WT at the different seedling stages, revealing that *rabc1-1* and *rabc1-2* were comparatively smaller than WT (Fig. 3b). Its root length and seedling biomass were also significantly reduced compared to WT (Fig. 3c, and d). Comparative phenotypic analysis at later stages of plant growth showed that the development of *rabc1-1* and *rabc1-2* lines was slow compared to WT (Fig. 3e). We also observed a delayed flowering phenotype in the later stage of plant growth in *rabc1-1* and *rabc1-2* (Fig. 3f). Collectively, reduced root length, less biomass, and delayed flowering suggest that *RabC1* is involved in multiple developmental pathways through controlling the vesicle trafficking events.

RabC1 expression was seen in the seed tissue during seed development, including chalazal endosperm, funiculus, chalazal seed coat, and embryo (Fig. 2m, and n). We observed that the seed size of *rabc1-1* and *rabc1-2* was significantly smaller than WT (Fig. 4a). Quantitative seed size and mass analysis further validate the results (Fig. 4b, c, d, e, f, and g). Numerous studies suggest that multiple sugar and amino acid transporters play a crucial role in seed filling and thus govern seed size (Chen et al. 2012, 2015; Mu et al. 2015; Besnard et al. 2018). The expression of *SWEET11* and *SWEET15* was significantly downregulated in *rabc1-2* seeds (Fig. 4h). The reported GUS expression pattern of *SWEET11* in leaves and seeds (Chen et al. 2012, 2015) was highly similar to the *RabC1* (Fig. 2b, c, and d). However, further work is needed to validate the relation between *RabC1* and *SWEET* genes. Similarly, the expression of amino acid transporters *UMAMIT24* and *UMAMIT25* was also significantly downregulated in *rabc1-2* seeds (Fig. 4h). *UMAMIT24* and

UMAMIT25 are expressed in the chalazal seed coat in developing seeds and help transport amino acids from maternal tissue to seeds through the chalazal seed coat (Besnard et al. 2018). The above findings indicate that the transportation of amino acids in the seed and the seed-filling process were affected by the disruption of RabC1 GTPase signaling.

The *rabc1-2* has a reduced endosperm cavity and smaller integument cell length, contributing to the smaller seed size (Fig. 5a). We observed lesser expansion in the integument cell wall of *rabc1-2* compared to WT (Fig. 5b). The reduction in the endosperm cavity area and integument cell length expansion in different stages of developing seeds further validates and illustrates the role of *RabC1* in seed development (Fig. 5c, and d). Together, the above results suggest that disruption of trafficking events leads to failure in the coordination among the seed tissues, i.e., embryo, seed coat, and endosperm that made the seed smaller, considering the role of Rab GTPase in nutrient transport. Furthermore, the percentage of tetrazolium red stained seeds was significantly high in *rabc1-2*, indicating that seed coat integrity was compromised in *rabc1-2* (Fig. 6a, and b), and RabC1 plays a role in regulating seed size and seed coat integrity.

The above results were further verified by restoring the mutant phenotype in the complementation line (Fig. 7, S8, and S9). A recent study suggests that TERMINAL FLOWER 1 (TFL1) plays a vital role in flowering and seed size regulation as its loss-of-function mutants also exhibited early flowering and prominent seed size phenotype (Zhang et al. 2020). The *rabc1-2* mutant showed smaller seed size and delayed flowering, and those phenotypic developmental defects were rescued in the complementation line (Fig. 7, S8, and S9). Thus, our results also suggest that RabC1 is involved in processes affecting both seed size and flowering.

Seed coat epidermal cells, which develop from the outer ovule integument, produce mucilage in *Arabidopsis*. The synthesis of cellulose occurs on the plasma membrane, while pectin and hemicelluloses are formed within the Golgi apparatus, which are eventually secreted to the apoplast (Young et al. 2008; Zhang et al. 2022). Plasma membrane-localized cellulose synthase (CESA) complexes are necessary for cellulose biosynthesis and cell wall formation. The synthesis and assembly of CESA proteins occur in the endoplasmic reticulum and Golgi. Hence, the trafficking of these complexes between organelles and their regulation is crucial for proper cell wall formation. Reportedly, Rab GTPase, such as Golgi localized RabH1b, is involved in the trafficking of CESAs to the plasma membrane (He et al. 2018).

Interestingly, we confirmed that the impairment of RabC1 function affects the secretion or deposition of mucilage. We observed reduced staining of ruthenium red in the *rabc1-2*, which depicted the declined pectin content (Fig. 8e). Additionally, reduced calcofluor staining in the *rabc1-2* showed decreased cellulose content (Fig. 8f). The

defective phenotype gets restored in the complementation line (Fig. 8e, and f). Overall, this result implies that RabC1 is involved in the trafficking of seed mucilage components.

Altogether, our work demonstrates the role of abundantly expressed *RabC1* in plant growth and especially in seed development. We showed that *RabC1* generates different isoforms to perform the function. RabC1 regulates root length and flowering time and is also involved in the regulation of seed size and seed filling process by affecting unknown steps of vesicle trafficking during seed development. Further detailed work is required to uncover the molecular characterization of *RabC1* that will help in the deep understanding of Rab GTPase signaling during growth and seed development. While this article was under review, a publication on RabC1 regarding its role in stomatal development was published (Ge et al. 2022). Similar to our work (Figs. 3 and 7), Ge et al. 2022 showed lesser biomass and reduced plant height in RabC1 (*lds1*) mutant, a single amino acid substitution mutant. In contrast, seed mass in the *lds1* mutant was unaffected compared to WT, compared to our results on T-DNA insertional knock-out mutant *rabc1-2* (Fig. 4), which showed lesser biomass than WT. Since we used knock-out mutant *rabc1-2* compared to their single amino acid substitution mutant *lds1*, this could be a possible reason for the contrasting results obtained in both studies.

Author contribution statement UK designed and performed all the experiments. First draft manuscript prepared by UK. SVS and VP supervised the study. SVS and UK analyzed and wrote the final manuscript. All authors read and approved the manuscript.

Supplementary Information The online version contains supplementary material available at <https://doi.org/10.1007/s00425-023-04122-2>.

Acknowledgements This work was supported by a grant from the Department of Biotechnology (DBT), India (Project Code, GAP-3361). We acknowledge the Director, CSIR-NBRI, for the resources and assistance. In addition, UK acknowledges the Department of Science and Technology, Government of India, for a research fellowship (DST/ INSPIRE Fellowship/2015/IF150279), and the University of Lucknow, Lucknow, U.P, India for Ph.D. registration. The institution manuscript number allotted to this manuscript is CSIR-NBRI_MS/2022/07/11.

Availability of data and materials All data generated or analyzed during this study are provided in this published article and its supplementary data files.

Declarations

Conflict of interest The authors declare no conflict of interest.

References

- Ambastha V, Matityahu I, Tidhar D, Leshem Y (2021) RabA2b over-expression alters the plasma-membrane proteome and improves drought tolerance in *Arabidopsis*. *Front Plant Sci* 12:738694. <https://doi.org/10.3389/fpls.2021.738694>
- Batoko H, Zheng HQ, Hawes C, Moore I (2000) A Rab1 GTPase is required for transport between the endoplasmic reticulum and Golgi apparatus and for normal Golgi movement in plants. *Plant Cell* 12:2201–2217. <https://doi.org/10.1105/tpc.12.11.2201>
- Besnard J, Zhao C, Avice J et al (2018) *Arabidopsis* UMAMIT24 and 25 are amino acid exporters involved in seed loading. *J Exp Bot* 69:5221–5232. <https://doi.org/10.1093/jxb/ery302>
- Chen PY, Wang CK, Soong SC, To KY (2003) Complete sequence of the binary vector pBI121 and its application in cloning T-DNA insertion from transgenic plants. *Mol Breed* 11:287–293. <https://doi.org/10.1023/A:1023475710642>
- Chen LQ, Qu XQ, Hou BH et al (2012) Sucrose efflux mediated by SWEET proteins as a key step for phloem transport. *Science* 80(335):207–211. <https://doi.org/10.1126/science.1213351>
- Chen L, Lin IW, Qu X et al (2015) A cascade of sequentially expressed sucrose transporters in the seed coat and endosperm provides nutrition for the *Arabidopsis* embryo. *Plant Cell* 27:607–619. <https://doi.org/10.1105/tpc.114.134585>
- Chen C, Chen H, Zhang Y et al (2020) TBtools: an integrative toolkit developed for interactive analyses of big biological data. *Mol Plant* 13:1194–1202. <https://doi.org/10.1016/j.molp.2020.06.009>
- Cheung AY, Chen CY, Glaven RH et al (2002) Rab2 GTPase regulates vesicle trafficking between the endoplasmic reticulum and the Golgi bodies and is important to pollen tube growth. *Plant Cell* 14:945–962. <https://doi.org/10.1105/tpc.000836.brane>
- Clough SJ, Bent AF (1999) Floral Dip : a Simplified Method for Agrobacterium-Mediated Transformation of *Arabidopsis* Thaliana. *Plant J* 16:735–743
- Creff A, Brocard L, Ingram G (2015) A mechanically sensitive cell layer regulates the physical properties of the *Arabidopsis* seed coat. *Nat Commun* 6:6382. <https://doi.org/10.1038/ncomms7382>
- De Graaf BHJ, Cheung AY, Andreyeva T et al (2005) Rab11 GTPase-regulated membrane trafficking is crucial for tip-focused pollen tube growth in tobacco. *Plant Cell* 17:2564–2579. <https://doi.org/10.1105/tpc.105.033183>
- Denay G, Creff A, Moussu S et al (2014) Endosperm breakdown in *Arabidopsis* requires heterodimers of the basic helix-loop-helix proteins ZHOUPI and INDUCER OF CBP EXPRESSION 1. *Development* 141:1222–1227. <https://doi.org/10.1242/dev.103531>
- Ebine K (2015) Roles of membrane trafficking in plant cell wall dynamics. *Front Plant Sci* 6:878. <https://doi.org/10.3389/fpls.2015.00878>
- Eisenberg E, Levanon EY (2003) Human housekeeping genes are compact. *Trends Genet* 19:2001–2004. [https://doi.org/10.1016/S0168-9525\(03\)00137-9](https://doi.org/10.1016/S0168-9525(03)00137-9)
- Foucart C, Moore I, Chow C (2008) Rab-A2 and Rab-A3 GTPases define a *trans*-Golgi endosomal membrane domain in *Arabidopsis* that contributes substantially to the cell plate. *Plant Cell* 20:101–123. <https://doi.org/10.1105/tpc.107.052001>
- Geldner N, Firml J, Stierhof YD et al (2001) Auxin transport inhibitors block PIN1 and vesicle trafficking. *Nature* 413:425–428
- Ge S, Zhang R-X, Wang Y-F, Sun P, Chu J, Li J, Sun P, Wang J, Hetherington AM, Liang Y-K (2022) The *Arabidopsis* Rab protein RABC1 affects stomatal development by regulating lipid droplet dynamics. *Plant Cell* 34(11):4274–4292. <https://doi.org/10.1093/plcell/koac239>
- Gu X, Brennan A, Wei W et al (2020) Vesicle transport in plants : a revised phylogeny of SNARE proteins. *Evol Bioinformatic* 16:1–11. <https://doi.org/10.1177/176934320956575>
- Harpaz-Saad S, McFarlane HE, Xu S et al (2011) Cellulose synthesis via the FEI2 RLK/SOS5 pathway and CELLULOSE SYNTHASE 5 is required for the structure of seed coat mucilage in *Arabidopsis*. *Plant J* 68:941–953. <https://doi.org/10.1111/j.1365-313X.2011.04760.x>
- Hashimoto K, Igarashi H, Mano S et al (2008) An isoform of *Arabidopsis* myosin XI interacts with small GTPases in its c-terminal tail region. *J Exp Bot* 59:3523–3531. <https://doi.org/10.1093/jxb/ern202>
- He M, Lan M, Zhang B et al (2018) Rab-H1b is essential for trafficking of cellulose synthase and for hypocotyl growth in *Arabidopsis thaliana*. *J Integr Plant Biol* 60:1051–1069. <https://doi.org/10.1111/jipb.12694>
- Higo K, Ugawa Y, Iwamoto M, Korenaga T (1999) Plant cis-acting regulatory DNA elements (PLACE) database : 1999. *Nucleic Acids Res* 27:297–300
- Huang F, Chi S, Chien P et al (2021) *Arabidopsis* RAB8A, RAB8B and RAB8D proteins interact with several RTNLB proteins and are involved in the *Agrobacterium tumefaciens* infection process. *Plant Cell Physiol* 62:1572–1588
- Jefferson RA, Kavanagh TA, Bevan MW (1987) GUS fusions: beta-glucuronidase as a sensitive and versatile gene fusion marker in higher plants. *EMBO J* 6:3901–3907
- Jia P, Xue Y, Li H, Yang W (2018) Golgi-localized LOT regulates trans-Golgi network biogenesis and pollen tube growth. *Proc Natl Acad Sci USA* 115:12307–12312. <https://doi.org/10.1073/pnas.1809206115>
- Kesari R, Lasky JR, Grace J et al (2012) Intron-mediated alternative splicing of *Arabidopsis* P5CS1 and its association with natural variation in proline and climate adaptation. *Proc Natl Acad Sci USA* 109:9197–9202. <https://doi.org/10.1073/pnas.1203433109>
- Khan D, Millar JL, Girard IJ et al (2015) Transcriptome atlas of the *Arabidopsis funiculosus*—a study of maternal seed subregions. *Plant J* 82(1):41–53. <https://doi.org/10.1111/tpj.12790>
- Kim D, Kim J, Baek D (2014) Global and local competition between exogenously introduced microRNAs and endogenously expressed microRNAs. *Mol Cells* 37:412–417
- Kirchhelle C, Chow CM, Foucart C et al (2016) The specification of geometric edges by a plant Rab GTPase is an essential cell-patterning principle during organogenesis in *Arabidopsis*. *Dev Cell* 36:386–400. <https://doi.org/10.1016/j.devcel.2016.01.020>
- Kotzer AM, Brandizzi F, Neumann U et al (2004) AtRabF2b (Ara7) acts on the vacuolar trafficking pathway in tobacco leaf epidermal cells. *J Cell Sci* 117:6377–6389. <https://doi.org/10.1242/jcs.01564>
- Lescot M, Déhais P, Thijs G et al (2002) PlantCARE, a database of plant cis-acting regulatory elements and a portal to tools for in silico analysis of promoter sequences. *Nucl Acids Res* 30:325–327
- Lianoglou S, Garg V, Yang JL et al (2013) Ubiquitously transcribed genes use alternative polyadenylation to achieve tissue-specific expression. *Genes Dev* 27:2380–2396. <https://doi.org/10.1101/gad.229328.113>
- Livak KJ, Schmittgen TD (2001) Analysis of relative gene expression data using real-time quantitative PCR and the 2- $\Delta\Delta CT$ method. *Methods* 25:402–408. <https://doi.org/10.1006/meth.2001.1262>
- Markgraf DF, Peplowska K, Ungermann C (2007) Rab cascades and tethering factors in the endomembrane system. *FEBS Lett* 581:2125–2130
- Maston GA, Evans SK, Green MR (2006) Transcriptional regulatory elements in the human genome. *Annu Rev Genom Hum Genet* 7:29–59. <https://doi.org/10.1146/annurev.genom.7.080505.115623>
- Mayers JR, Hu T, Wang C et al (2017) SCD1 and SCD2 form a complex that functions with the exocyst and RabE1 in exocytosis and cytokinesis. *Plant Cell* 29:2610–2625. <https://doi.org/10.1105/tpc.17.00409>

- Mayr C (2017) Regulation by 3-untranslated regions. *Annu Rev Genet* 51(1):171–194
- Mishra DK, Srivastava R, Pandey BK et al (2022) Identification and validation of the wound and insect bite early inducible promoter from *Arabidopsis thaliana*. *3 Biotech* 12:74. <https://doi.org/10.1007/s13205-022-03143-0>
- Mu B, Fastner A, Karmann J et al (2015) Amino acid export in developing *Arabidopsis* seeds depends on UmamiT facilitators. *Curr Biol* 25:3126–3131. <https://doi.org/10.1016/j.cub.2015.10.038>
- Nguyen H, Brown RC, Lemmon BE (2000) The specialized chalazal endosperm in *Arabidopsis thaliana* and *Lepidium virginicum* (Brassicaceae). *Protoplasma* 212:99–110
- Nielsen E (2020) The small GTPase superfamily in plants : a conserved regulatory module with novel functions. *Annu Rev Plant Biol* 71:247–272
- Olkonen VM, Stenmark H (1997) Role of Rab GTPases in membrane traffic. *Int Rev Cytol* 176:1–85
- Peng J, Ilarslan H, Wurtele ES, Bassham DC (2011) AtRabD2b and AtRabD2c have overlapping functions in pollen development and pollen tube growth. *BMC Plant Biol* 11:25. <https://doi.org/10.1186/1471-2229-11-25>
- Pereira-Leal JB, Seabra MC (2001) Evolution of the Rab family of small GTP-binding proteins. *J Plant Biol* 313:889–901. <https://doi.org/10.1006/jmbi.2001.5072>
- Prasad P, Khatoon U, Verma RK et al (2022) Transcriptional landscape of cotton fiber development and its alliance with fiber-associated traits. *Front Plant Sci* 13:811655. <https://doi.org/10.3389/fpls.2022.811655>
- Preuss ML, Serna J, Falbel TG et al (2004) The *Arabidopsis* Rab GTPase RabA4b localizes to the tips of growing root hair cells. *Plant Cell* 16:1589–1603. <https://doi.org/10.1105/tpc.021634.tip-localized>
- Ren D, Wang X, Yang M et al (2019) A new regulator of seed size control in *Arabidopsis* identified by a genome-wide association study. *New Phytol* 1:895–906. <https://doi.org/10.1111/nph.15642>
- Rojo E, Gillmor CS, Kovaleva V et al (2001) VACUOLELESS1 is an essential gene required for vacuole formation and morphogenesis in *Arabidopsis*. *Dev Cell* 1:303–310
- Rutherford S, Moore I (2002) The *Arabidopsis* Rab GTPase family: another enigma variation. *Curr Opin Plant Biol* 5:518–528
- Srivastava R, Rai KM, Srivastava M et al (2014) Distinct role of core promoter architecture in regulation of light-mediated responses in plant genes. *Mol Plant* 7:626–641. <https://doi.org/10.1093/mp/sst146>
- Stenmark H (2009) Rab GTPases as coordinators of vesicle traffic. *Nat Publ Gr* 10:513–525. <https://doi.org/10.1038/nrm2728>
- Stenmark H, Parton RG, Steele-mortimer O, Lutcke A (1994) Inhibition of Rab5 GTPase activity stimulates membrane fusion. *EMBO J* 13:1287–1296
- Szumlanski AL, Nielsen E (2009) The Rab GTPase RabA4d regulates pollen tube tip growth in *Arabidopsis thaliana*. *Plant Cell* 21:526–544. <https://doi.org/10.1105/tpc.108.060277>
- Takano J, Miwa K, Yuan L et al (2005) Endocytosis and degradation of BOR1, a boron transporter of *Arabidopsis thaliana*, regulated by boron availability. *Proc Natl Acad Sci USA* 102:12276–12281. <https://doi.org/10.1073/pnas.0502060102>
- Vernoud V, Horton AC, Yang Z, Nielsen E (2003) Analysis of the small GTPase gene superfamily of *Arabidopsis*. *Plant Physiol* 131:1191–1208. <https://doi.org/10.1104/pp.013052>
- Wang W, Sun K, Zhang B, Wang W (2021) New insights into cell–cell communications during seed development in flowering plants. *J Integr Plant Biol* 64:215–229. <https://doi.org/10.1111/jipb.13170>
- Wang L, Li D, Yang K et al (2022) Connected function of PRAF/RLD and GNOM in membrane trafficking controls intrinsic cell polarity in plants. *Nat Commun* 13:7. <https://doi.org/10.1038/s41467-021-27748-w>
- Weigel D, Mott R (2009) The 1001 genomes project for *Arabidopsis thaliana*. *Genome Biol* 10:107. <https://doi.org/10.1186/gb-2009-10-5-107>
- Willats WGT, McCartney L, Knox JP (2001) In-situ analysis of pectic polysaccharides in seed mucilage and at the root surface of *Arabidopsis thaliana*. *Planta* 213:37–44
- Winter D, Vinegar B, Nahal H et al (2007) An “electronic fluorescent pictograph” browser for exploring and analyzing large-scale biological data sets. *PLoS ONE* 2:e718. <https://doi.org/10.1371/journal.pone.0000718>
- Woollard AA, Moore I (2008) The functions of Rab GTPases in plant membrane traffic. *Curr Opin Plant Biol* 11:610–619
- Young RE, McFarlane HE, Hahn MG et al (2008) Analysis of the Golgi apparatus in *Arabidopsis* seed coat cells during polarized secretion of pectin-rich mucilage. *Plant Cell* 20:1623–1638. <https://doi.org/10.1105/tpc.108.058842>
- Zerial M, McBride H (2001) Rab proteins as membrane organizers. *Nat Rev Mol Cell Biol* 2:107–117
- Zhang Y, Zhang B, Yan D et al (2011) Two *Arabidopsis* cytochrome P450 monooxygenases, CYP714A1 and CYP714A2, function redundantly in plant development through gibberellin deactivation. *Plant J* 53:342–353. <https://doi.org/10.1111/j.1365-313X.2011.04596.x>
- Zhang B, Li C, Li Y, Yu H (2020) Mobile TERMINAL FLOWER1 determines seed size in *Arabidopsis*. *Nat Plants* 6:1146–1157. <https://doi.org/10.1038/s41477-020-0749-5>
- Zhang Y, Yin Q, Qin W et al (2022) The Class II KNOX family members KNAT3 and KNAT7 redundantly participate in *Arabidopsis* seed coat mucilage biosynthesis. *J Exp Bot* 73:3477–3495. <https://doi.org/10.1093/jxb/erac066>
- Zheng H, Camacho L, Wee E et al (2005) A Rab-E GTPase mutant acts downstream of the Rab-D subclass in biosynthetic membrane traffic to the plasma membrane in tobacco leaf epidermis. *Plant Cell* 17:2020–2036. <https://doi.org/10.1105/tpc.105.031112>
- Zheng D et al (2018) Cellular stress alters 3'UTR landscape through alternative polyadenylation and isoform-specific degradation. *Nat Commun* 9:1–14
- Zhou Y, Yang Y, Niu Y et al (2020) The tip-localized phosphatidylserine established by *Arabidopsis* ALA3 is crucial for Rab GTPase-mediated vesicle trafficking and pollen tube growth. *Plant Cell* 32:3170–3187. <https://doi.org/10.1105/tpc.19.00844>

Publisher's Note Springer Nature remains neutral with regard to jurisdictional claims in published maps and institutional affiliations.

Springer Nature or its licensor (e.g. a society or other partner) holds exclusive rights to this article under a publishing agreement with the author(s) or other rightsholder(s); author self-archiving of the accepted manuscript version of this article is solely governed by the terms of such publishing agreement and applicable law.